

## Electronic Supplementary Information

### **Rheoreversible metallosupramolecular soft-nanostructure of Cd(II) for fabricating thin-film based semiconducting device**

Supravat Ghosh,<sup>a</sup> Indrajit Pal,<sup>b</sup> Amiya Dey,<sup>b,c</sup> Suresh Kumar Yatirajula,<sup>d</sup> Partha Pratim Ray,<sup>a,\*</sup> Biswajit Dey<sup>b,\*</sup>

<sup>a</sup>Department of Physics, Jadavpur University, Kolkata-700032, India, E-mail: parthap.ray@jadavpuruniversity.in (P.P.R.)

<sup>b</sup>Department of Chemistry, Visva-Bharati University, Santiniketan-731235, India, E-mail: bdeychem@gmail.com, biswajit.dey@visva-bharati.ac.in (B.D.)

<sup>c</sup>Department of Chemistry, Netaji Subhas University, Jamshedpur, 831012, India

<sup>d</sup>Department of Chemical Engineering, Indian Institute of Technology (Indian School of Mines), Dhanbad, 826004, Jharkhand, India

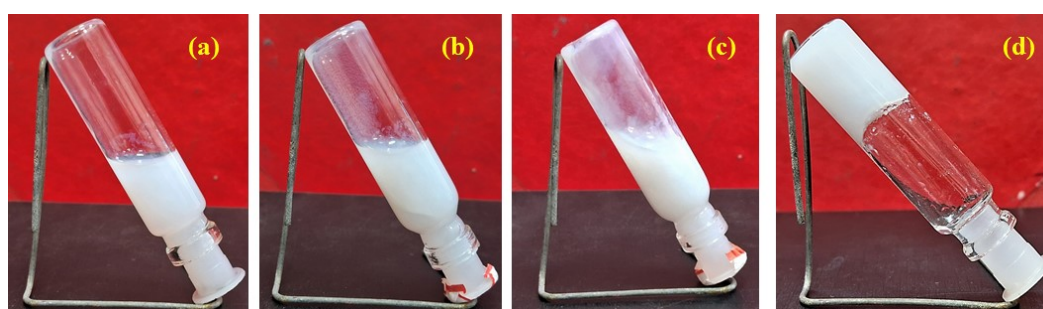
### 1. Determination of Minimum Critical Gelation (MCG) Concentration for the synthesized Cd-PDCA metallogel.

Minimum critical gel concentration (MCG) of Cd(II) source, and 2,6-pyridinedicarboxylic acid-directed Cd-PDCA metallogel was examined (Fig. S1). For Cd-PDCA metallogel, the concentrations of gel-forming chemical components i.e.,  $\text{Cd}(\text{CH}_3\text{COO})_2 \cdot 2\text{H}_2\text{O}$ , and 2,6-pyridinedicarboxylic acid were reserved as 1:1 molar ratio. Following this stoichiometric feature, the concentration of Cd(II) metal salt, and organic gelator i.e., 2,6-pyridinedicarboxylic acid, were varied to determine the MCG in the polar aprotic solvent medium like DMF (different concentrations are tabulated as Table S1).

The finest quality supramolecular metallogel of Cd-PDCA metallogel was experientially obtained at the certain values of minimum concentrations for Cd(II)-acetate dihydrate, and 2,6-pyridinedicarboxylic acid as 0.0799, and 0.0501 g/ml, respectively.

**Table S1.** Determination of Minimum Critical Gelation (MCG) concentration of Cd-PDCA metallogel.






















Serial No.	Amount used for every gel-forming chemical-constituent (in mM)	$\text{Cd}(\text{CH}_3\text{COO})_2 \cdot 2\text{H}_2\text{O}$ (in 1ml DMF) (in g)	2,6-pyridinedicarboxylic acid (in 1ml DMF) (in g)	Phase
(a)	0.05	0.0133	0.0083	Sol
(b)	0.1	0.0266	0.0167	Sol
(c)	0.2	0.0533	0.0334	Viscous sol
(d)	0.3	0.0799	0.0501	Gel



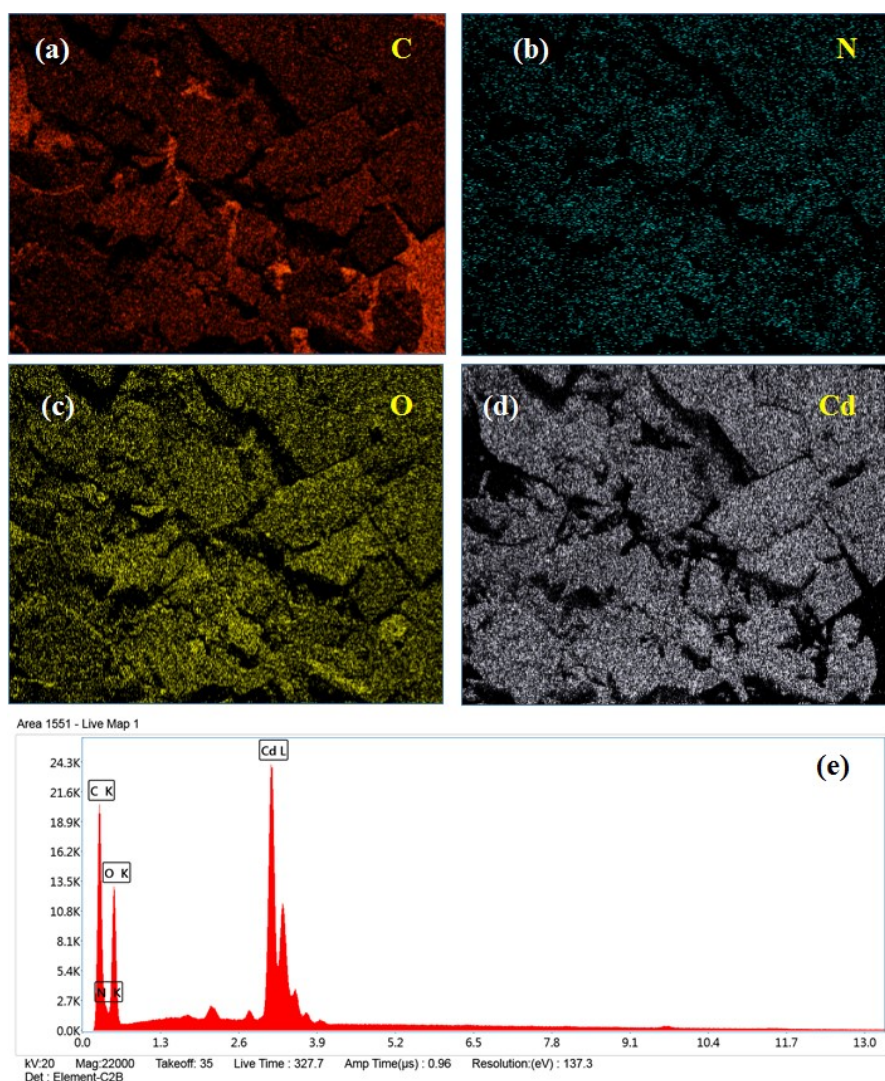
**Fig. S1.** Determination of Minimum Critical Gelation (MCG) concentration of Cd-PDCA metallogel. Here, (a)-(d) stand for stepwise images of Cd-PDCA metallogel by using metallogel-forming chemical constituents with different concentrations. Details of concentrations as given in Fig. S1 a, b, c, d are documented in different entries of Table S1 (i.e., entries like a, b, c, and d, respectively).

**2. Optimization study: Effect of different solvents and Cd(II) metal salts with diverse counter anions.**

**Table S2.** Testing of metallogelation process for different solvents and Cd(II) metal salts with diverse counter anions.

Solvents	$\text{Cd}(\text{OAc})_2 \cdot 2\text{H}_2\text{O}$	$\text{Cd}(\text{NO}_3)_2 \cdot 4\text{H}_2\text{O}$	$\text{CdCl}_2$	$\text{CdBr}_2 \cdot 4\text{H}_2\text{O}$
$\text{CH}_3\text{COOH}$				
$\text{CHCl}_3$				
$\text{CH}_3\text{COOC}_2\text{H}_5$				
$\text{H}_2\text{O}$				
$\text{CH}_3\text{CN}$				
PET				
THF				

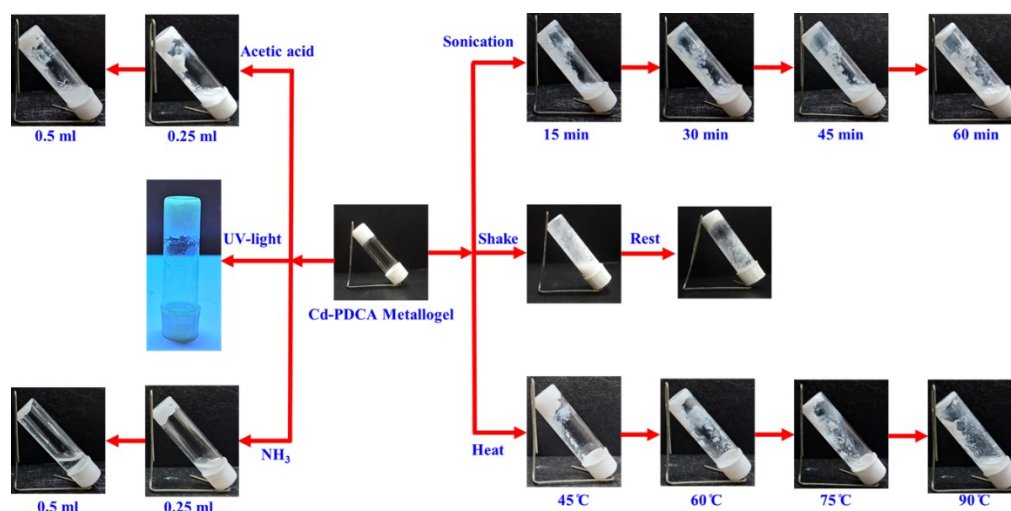
### 3. Microstructural elemental mapping of Cd-PDCA metallogel.



**Fig. S2.** EDS elemental analyses of Cd-PDCA metallogel indicating the existence of elements: (a) C, (b) N, (c) O, and (d) Cd; (e) represents the EDX spectrum of Cd-PDCA metallogel.



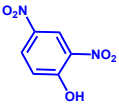
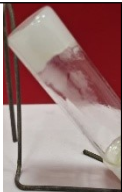



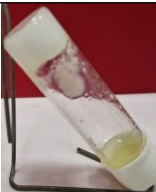

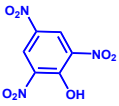


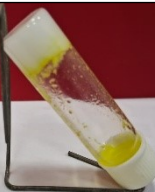
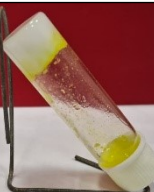
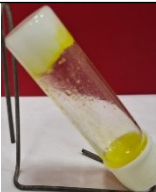

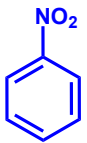
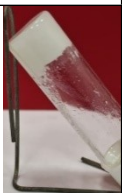



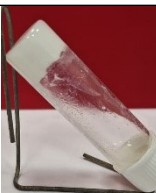
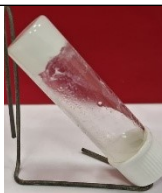







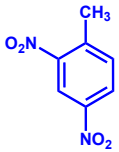
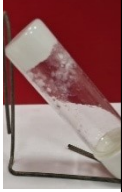




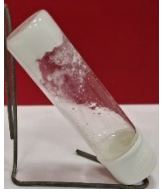
#### 4. Stimuli-responsive study of Cd-PDCA metallogel.



**Fig. S3.** Stimuli-responsive study of Cd-PDCA metallogel, by implementing ultrasonication (See Electronic supplementary information for the results of different time intervals), mechanical shaking by vortex, heating effect (See Electronic supplementary information for the results of metallogel exposing under applied increasing temperatures), different amount of ammonia solution, and acetic acid solution, and fluorescent behaviour through UV-light exposure.

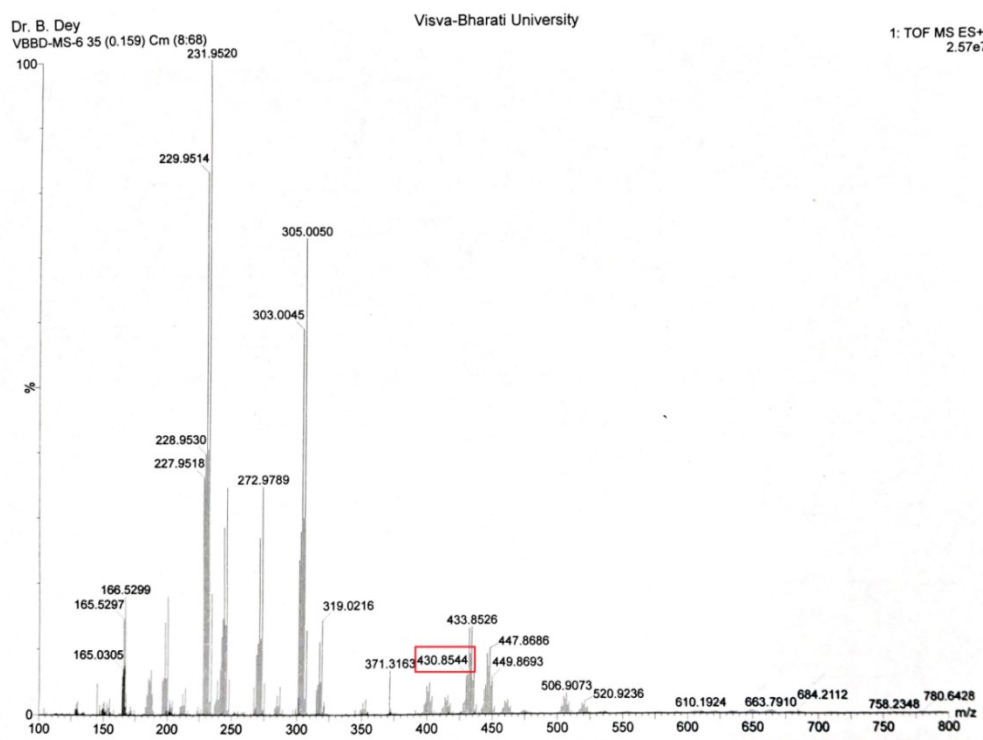
**Table S3.** Finding the impact of different nitrophenols and nitro-aromatic compounds toward Cd-PDCA metallogel through individual attempts.

Chemical-stimuli	Volume of chemical stimuli added					
	50 $\mu\text{L}$	100 $\mu\text{L}$	200 $\mu\text{L}$	300 $\mu\text{L}$	400 $\mu\text{L}$	500 $\mu\text{L}$

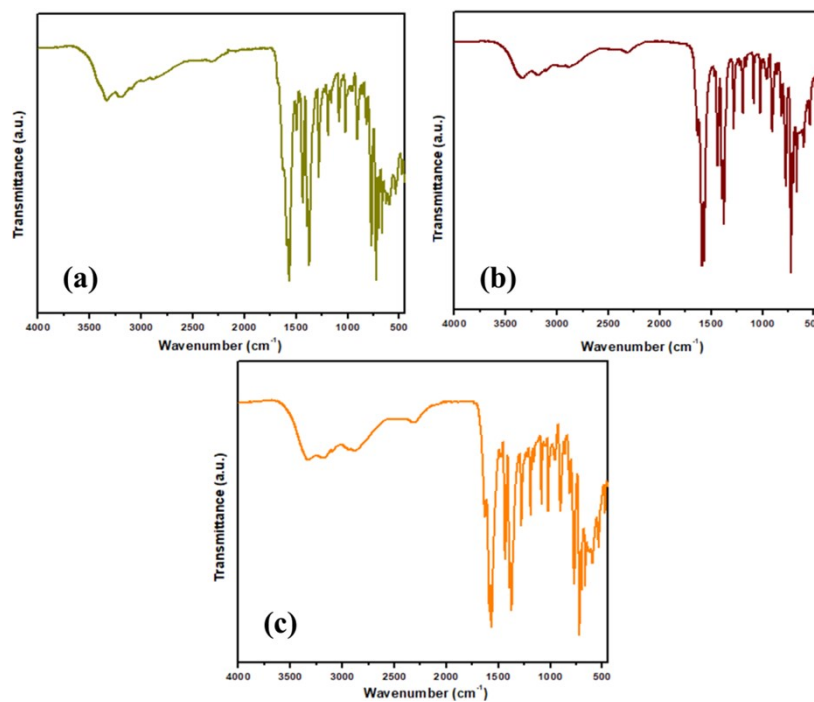
(here, [nitro-compound] = 5 mM)

## 5. ESI-Mass spectrometric analyses of Cd-PDCA metallogel.



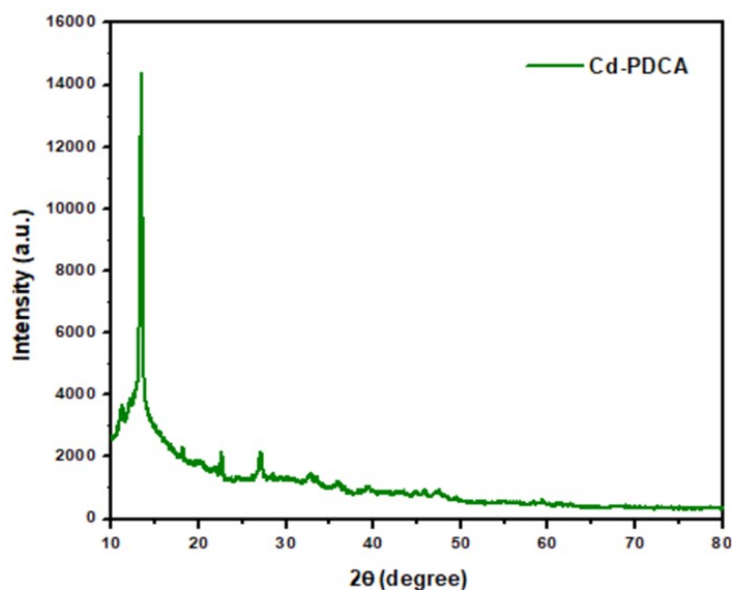
**Fig. S4.** ESI-Mass spectra of Cd-PDCA metallogel.

## 6. FTIR study of Cd-PDCA metallogel after interacting with different amines.



**Fig. S5.** FT-IR analyses of Cd-PDCA metallogel after interacting with different amines: (a) 2-aminopyridine, (b) 2-aminopyrimidine, and (c) 2-(2-pyridyl)ethylamine.

## 7. PXRD study of Cd-PDCA metallogel.



**Fig. S6.** PXRD pattern of xerogel sample of Cd-PDCA metallogel.

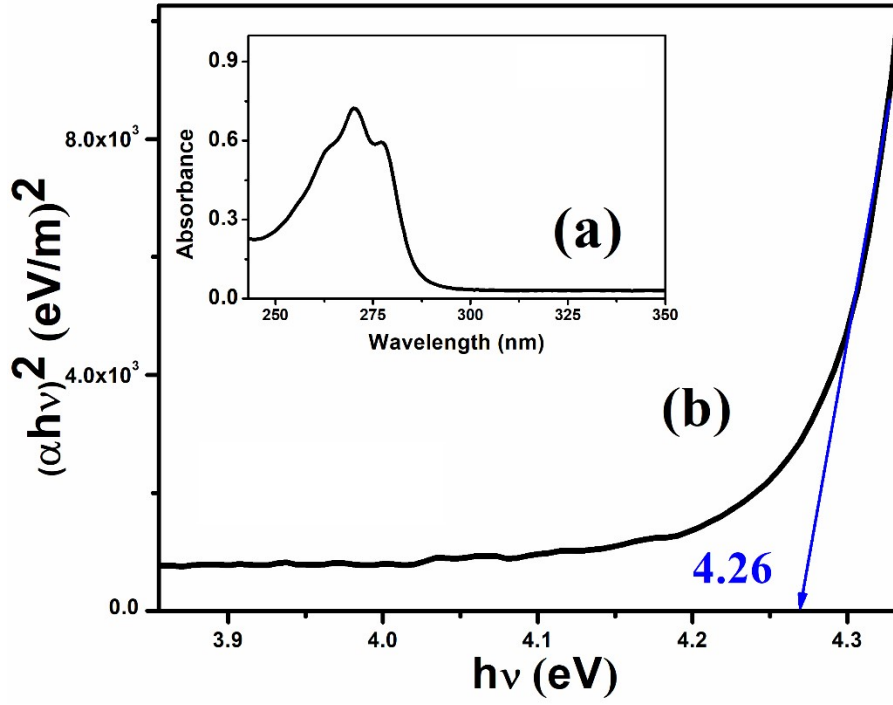
## 8. Optical characterization.

The absorption spectra were recorded by UV-Vis spectroscopy and respective Tauc's plots of synthesized metallogel are shown in Fig. S7. The optical band gap of the complexes has been estimated with the help of Tauc's equation (Equation S1).

$$(\alpha h\nu)^n = A(h\nu - E_g) \quad (S1)$$

where  $\alpha$  is the absorption coefficient,  $E_g$  is the optical band gap energy,  $h$  is Planck's constant,  $\nu$  is frequency,  $A$  is an arbitrary constant and  $n = 2$ , corresponding to the allowed direct electronic transitions.<sup>1,2</sup> The evaluated band gap energies, which correspond to the electronic transition energy from the valance band to conduction band, was 4.26 eV for the Cd-PDCA.





**Fig. S7.** (a) Absorbance spectra of metallogel (b) Tauc's plot for the direct band gap is shown in the inset for this metallogel.

### 9. Electrical Characterization.

The Thermionic Emission (TE) theory is adopted to get more insights of the charge transport mechanism in the devices.<sup>3</sup> The current of a diode can be expressed as the following equations according to TE theory (Equation S2).<sup>4</sup>

$$I = I_0 \exp\left(\frac{qV}{\eta kT}\right) \left[1 - \exp\left(-\frac{qV}{\eta kT}\right)\right] \quad (\text{S2})$$

Where,

$$I_0 = AA^* T^2 \exp\left(-\frac{q\phi_B}{kT}\right) \quad (\text{S3})$$

$$\phi_B = \frac{kT}{q} \ln\left(\frac{AA^* T^2}{I_0}\right) \quad (\text{S4})$$

Where,  $I_0$  indicates the saturation current,  $q$  represents the electronic charge,  $k$  is the Boltzmann constant,  $T$  is the temperature in Kelvin,  $V$  is the forward bias voltage,  $\eta$  is the ideality factor,  $\phi_B$  is the effective barrier height at zero bias,  $A$  is the diode area ( $7.065 \times 10^{-6} \text{ m}^2$ ),  $A^*$  is the effective Richardson constant ( $1.20 \times 10^6 \text{ Am}^{-2}\text{K}^{-2}$ ). From Cheung, the forward bias  $I$ - $V$  characteristics in term of series resistance can be expressed through Equation S5.<sup>5</sup>

$$I = I_0 \exp \left[ \frac{q(V - IR_s)}{\eta kT} \right] \quad (S5)$$

Where, the  $IR_s$  term represents the voltage drop across the series resistance of the device. In this circumstance, the values of the series resistance can be determined from the following functions using equation (S6 and S7).<sup>6</sup>

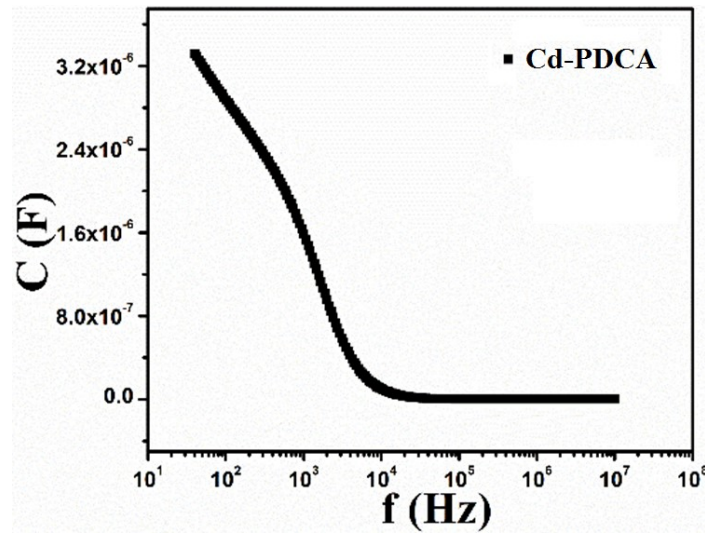
According to Cheung's model:

$$\frac{dV}{d \ln(I)} = \left( \frac{\eta kT}{q} \right) + R_s I \quad (S6)$$

$$H(I) = R_s I + \eta \phi_B \quad (S7)$$

and  $H(J)$  can be expressed via Equation S8.

$$H(I) = V - \left( \frac{\eta kT}{q} \right) \ln \left( \frac{I}{AA * T^2} \right) \quad (S8)$$



**Fig. S8.** Capacitance versus frequency plot for Cd-PDCA metallogel-based Device.

## References

- 1 J. Tauc, Amorphous and Liquid Semiconductors. *Plenum Press*, New York, 1974.
- 2 J. Datta, M. Das, S. Sil, S. Kumar, A. Dey, R. Jana, S. Bandyopadhyay and P. P. Ray, *Mater. Sci. Semicond. Process.*, 2019, **91**, 133-145.
- 3 E. H. Rhoderick and R. H. Williams, *Clarendon Press*, Oxford, 2nd edn, 1988.
- 4 S. M. Sze, *Wiley*, New York., 1981.
- 5 S. Sil, R. Jana, A. Biswas, D. Das, A. Dey, J. Datta, D. Sanyal and P. P. Ray, *IEEE Trans. Electron Devices*, 2020, **67**, 2082-2087.
- 6 M. Das, M. Das, S. Ray, U. K. Das, S. Laha, P. P. Ray, B. C. Samanta and T. Maity, *New J. Chem.*, 2022, **46**, 21103-21114.